



A comparative study for adsorption of methylene blue from aqueous solutions by two kinds of amberlite resin materials

Özge Kerkez*, Şahika Sena Bayazit, Hasan Uslu

*Engineering and Architecture Faculty, Chemical Engineering Department, Beykent University, Ayazağa, İstanbul, Turkey
Tel. +90 212 444 19 97 / 5294; email: ozgekerkez@beykent.edu.tr*

Received 8 September 2011; Accepted 27 November 2011

ABSTRACT

An organic dye, methylene blue (MB), was separated from a model aqueous solution by using adsorption method with low cost resin adsorbents. The adsorption of MB was studied with Amberlite XAD-16 and Amberlite XAD-7 HP. The aim of the study is to achieve a high removal value of the dye and comparing these two adsorbents for MB adsorption. Adsorption of MB was investigated in terms of equilibrium and kinetics conditions. Adsorption isotherms were determined and correlated with equations such as Freundlich, Langmuir and Temkin isotherm models. Langmuir isotherm has good agreement with R^2 value over 0.99. Pseudo second order model was fitted for this adsorption system. Here we showed that 99% removal of MB can be achieved with Amberlite XAD-16. SEM studies revealed the morphological observations of the unloaded adsorbent and the changes in the adsorbed polymeric resin. FTIR spectrums of adsorbents before and after the adsorption supported the SEM results.

Keywords: Methylene blue adsorption; Amberlite XAD-16; Amberlite XAD-7 HP; Freundlich; Langmuir; Temkin

1. Introduction

Existence of organic dyes in wastewater of textile industry is not desired from the point of view health and also aesthetic. Due to the high concentration of organics in the effluents and the higher stability of modern synthetic dyes, their discharges into nature are very harmful. Therefore removal of these organic dyes from wastewater is an important environmental problem.

Wastewaters and dangerous chemicals hard to degrade in wastewater are increasing with developing industry and technology. Wastewater treatment is important from the point of view consuming clean water sources and also due to constituting a serious threat for

health with discharging the wastewater to nature. Performing these treatment processes in an economical and efficient way is also very important.

Many wastewaters contain significant levels of organic contaminants, which are toxic because they create odor, unsightly color, foaming, etc. [1]. Dyes are widely used chemicals and consequently, these pollutants may be found in wastewaters of many industries dyes are widely used chemicals and consequently these pollutants may be found in wastewaters of many industries [2,3].

With increasing revolution in science and technology, there was a bigger demand on opting for newer chemicals which could be used in various industrial processes. Organic dyes came up as one of the many new chemicals which could be used in many industrial activities. Due

*Corresponding author.

to the extensive use of these dyes in industries, they have become an integral part of industrial effluent. According to a review study in 2004, the amount of dyes produced in the world is estimated to be over 10,000 t y⁻¹. Exact data on the quantity of dyes discharged in the environment are also not available. It is assumed that a loss of 1–2% in production and 1–10% loss in use are a fair estimate. For reactive dyes, this figure can be about 4% [4]. The release of those colored wastewaters in the environment is a considerable source of non-aesthetic pollution and eutrophication and can originate dangerous byproducts through oxidation, hydrolysis, or other chemical reactions taking place in the wastewater phase [5]. Most of these dyes are toxic and potentially carcinogenic in nature and their removal from the industrial effluents is a major environmental problem. Indeed, it is necessary to eliminate them from wastewater before it is discharged.

Liquid phase adsorption process is highly efficient method for the removal of colors, odors, biological matter, and organic matter from process or waste effluents [6,7]. Activated carbons (ACs) are important materials known for their great ability to adsorb various molecules on their surface. Despite its frequent use, AC remains an expensive material [2]. Although ACs are among the most effective adsorbents and can be regenerated by thermal desorption or combustion of the pollutant in air, a substantial fraction of the carbon is lost with each regeneration cycle [1]. In the past two decades synthetic resin adsorbents have often been regarded as an alternative of activated carbon since they can be easily regenerated and chemical pollutants can be recovered after regeneration of the adsorbents [8].

Besides a lot of dye adsorption studies on the various carbon type adsorbents [9], there are several papers about methylene blue adsorption on the clays like kaolinite [10], sepiolite [11], perlite [12], zeolite [13], montmorillonite [14], bentonite [15]. Fungaro et al. studied methylene blue adsorption on zeolite synthesized from fly ash as different from other adsorbents [16]. Methylene blue adsorption equilibrium and kinetic parameters were determined for these adsorbents. Also a lot of studies about adsorption of reactive dyes on several adsorbents, for example Lin and Wang studied adsorption of different textile dyes on organically modified bentonite [17].

In the present study, the adsorption isotherms and kinetic models of methylene blue were investigated for two different structured resin adsorbents. The experimental data have been modeled by using the Langmuir, Freundlich and Temkin isotherms. The kinetic data obtained from the batch adsorption process were analyzed using the pseudo second order model, Elovich model and Weber Morris Intra-particle diffusion model.

2. Experimental

2.1. Materials

Methylene blue was obtained from Merck Co., Amberlite XAD-16 and Amberlite XAD-7 HP were obtained from Fluka Co. All chemicals and reagents used in this work had a pure analytical quality. It was used without further treatment. In all experiments, deionized water was used for preparation, dilution and analytical purposes of solutions.

2.2. Adsorption studies

The mixtures of known amount of adsorbent and 20 ml methylene blue solution was prepared and equilibrium was carried out in a thermostatic shaker. So, the period of equilibrium state for Amberlite XAD-16 was determined as approximately 30 h. The samples were shaken for 32 h and optimum amount of adsorbent was determined as 10 mg for Amberlite XAD-16. The period of equilibrium state for Amberlite XAD-7HP was determined as approximately 5 h. The samples were shaken for 5 h and optimum amount of adsorbent was determined as 10 mg for Amberlite XAD-7 HP.

Adsorption isotherms were obtained using the batch equilibrium technique. In adsorption processes, the concentration of the dye also plays an important role. For this investigation, the methylene blue adsorption on Amberlite XAD-16 and Amberlite XAD-7 HP was studied at a constant amount of resin 10 mg and varying methylene blue concentrations (0–15 mg l⁻¹) in the aqueous phase at room temperature by shaking until equilibrium state was achieved. Experimental data obtained from this study, were evaluated with Freundlich, Langmuir and Temkin isotherms models.

Adsorption experiments were performed by batch mode in conical flasks. First 10 mg resin samples were added to several 100 ml volumed flasks, a 20 ml aqueous solution containing known concentration of each adsorbate was then added into each flask. Afterwards the flasks were shaken at 120 rpm. At particular time intervals, shaking was stopped for a moment and sample solution was taken with a injection syringe, analyzed for MB.

2.3. Characterization of adsorptions

A stock solution of methylene blue was prepared in deionized water. Solutions with the desired concentrations (0–15 ppm) of methylene blue were prepared by successive dilutions of the stock solution.

The concentrations were analyzed using an UV–vis spectrophotometer at 665 nm for methylene blue. Linear calibration curve were used in the determination of concentrations. The curve were based on standards in the concentration range from 0 to 15 ppm.

The amounts adsorbed by resin particles at time t , q_t (mg g^{-1}), was calculated by:

$$q_t = \frac{V(C_0 - C_t)}{W} \quad (1)$$

where C_0 and C_t are the liquid concentrations at the start and at time t , respectively, V the volume of aqueous solution and W the mass of resin.

Methylene blue removal (%) was calculated using the following equation:

$$\text{MB removal (\%)} = \frac{C_0 - C_t}{C_0} \times 100 \quad (2)$$

Fourier transform infrared (FTIR) spectra were recorded using a Thermo Nicolet 380 spectrometer in the wave number range from 400 to 4000 cm^{-1} , with samples prepared by the KBr method, where the sample to KBr ratio was 1:100.

The surface characteristics of the pure and saturated Amberlite XAD-16 particles were analyzed by Field Emission Scanning Electron Microscopy (FE-SEM, FEI Quanta FEG 450). The sample was sputtered with gold and measured at an operation voltage of 20 kV.

3. Results and discussion

In this study, firstly the period of the equilibrium state of the adsorbents was determined in terms of the effect of amount of adsorbent, the effect of initial dye concentrations. According to equilibrium results some isotherms (Langmuir, Freundlich and Temkin) were applied to experimental data. Secondly, to determine order of adsorption process, the kinetic studies of methylene blue adsorption on both adsorbents were investigated.

3.1. Effect of amount of adsorbent

Under optimum conditions of shaking time, the effect of adsorbent dose on the extent of solute adsorption was investigated by varying approximately dose from 0.01 to 0.05 g of Amberlite XAD-16 and XAD-7 HP for 9.60 ppm initial methylene blue concentration at room temperature. The results are presented in Tables 1

Table 1
Effect of amount of XAD-16 on the adsorption of MB

Amount of XAD-16 (g)	C_0 (mg l^{-1})	C_e (mg l^{-1})	q_e	Removal (%)
0.01	9.60	1.60	13.55	83.25
0.02	9.60	0.39	7.77	95.88
0.03	9.60	0.20	6.06	97.87
0.04	9.60	0.03	4.61	99.70
0.05	9.60	0.05	3.62	99.48

Table 2
Effect of amount of XAD-7 HP on the adsorption of MB

Amount of XAD-7 (g)	C_0 (mg l^{-1})	C_e (mg l^{-1})	q_e	Removal (%)
0.01	9.60	8.58	1.82	10.64
0.02	9.60	6.97	2.34	27.38
0.03	9.60	5.63	2.43	41.33
0.04	9.60	4.85	2.25	49.48
0.05	9.60	3.86	2.21	59.76

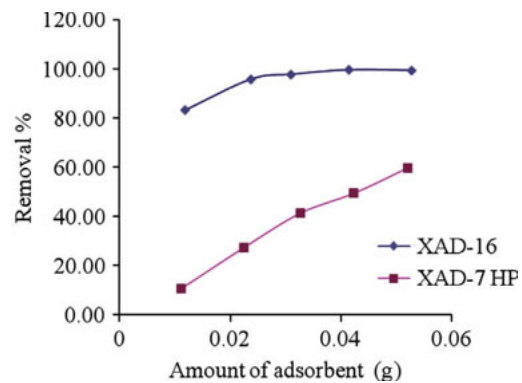


Fig. 1. Removal of methylene blue with different amount of adsorbents.

and 2 for XAD-16 and XAD-7 HP, respectively. It has been observed from Fig. 1 that as the dose increases the amount of solute adsorbed increases for both adsorbent. The maximum removals of methylene blue have been determined as 99% and 59% for approximately 0.05 g XAD-16 and XAD-7 HP of adsorbents, respectively.

3.2. Effect of initial dye concentration

Different initial MB concentrations (0.94, 5.35, 7.72, 10.18, 14.11 ppm) were studied for 10 mg XAD-16 and XAD-7 HP adsorbents. Results have been presented Tables 3 and 4. Fig. 2 shows that with the increasing of initial MB concentration from 0.94 to 14.11 ppm adsorbed amount of dye decreased due to decreased efficiency of

Table 3
Effect of initial MB concentration on the adsorption with XAD-16

Amount of XAD-16 (g)	C_0 (mg l^{-1})	C_e (mg l^{-1})	q_e	Removal (%)
0.01	0.94	0.001	1.89	99.99
0.01	5.35	0.03	9.86	99.43
0.01	7.72	0.13	14.46	98.26
0.01	10.18	0.85	18.49	91.69
0.01	14.11	2.35	21.37	83.31

Table 4
Effect of initial MB concentration on the adsorption with XAD-7 HP

Amount of XAD-7 (g)	C ₀ (mg l ⁻¹)	C _e (mg l ⁻¹)	q _e	Removal (%)
0.01	0.65	0.31	0.63	52.69
0.01	4.95	2.92	2.53	41.11
0.01	10.12	8.27	3.31	18.31
0.01	13.76	12.43	2.42	9.67

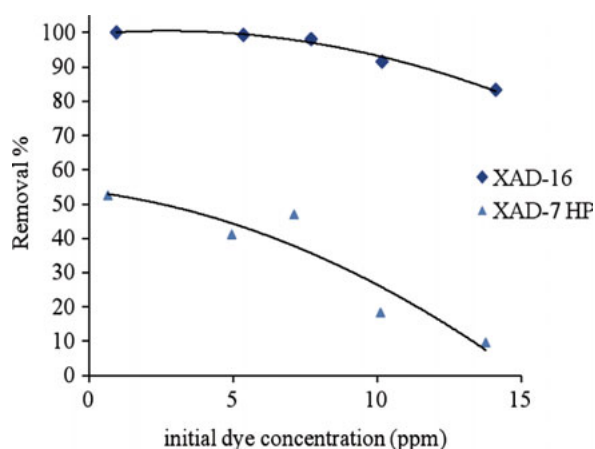


Fig. 2. Effect of initial concentration of MB on the adsorption.

XAD-16 and XAD-7 HP. Efficiency of removal decreased from 99.99% to 83.31% with the increased initial concentration of MB. At the same conditions in adsorption of MB with XAD-7 HP, the efficiencies have been decreased from 52.69% to 9.67%. This may be explained by the saturation of accessible exchangeable sites of these adsorbents.

3.3. Isotherms

Langmuir isotherm, Freundlich isotherm and Temkin isotherm were studied to find equilibrium characteristics of the adsorption.

The Langmuir equation [18,19]:

$$q_e = \frac{K_A \cdot Q_m \cdot C_e}{1 + K_A \cdot C_e} \quad (1)$$

q_e denote the adsorbent-phase concentrations of MB and Q_m a partial limiting adsorption capacity when the surface is fully covered with dye molecules that assists in the comparison of adsorption performance (saturation capacity). K_A is the equilibrium constant or Langmuir constant related to the affinity of binding sites (l mg⁻¹) or (l mol⁻¹).

The values of K_A and Q_m are determined by the following equation to which Eq. (2) is transformed:

$$\frac{C_e}{q_e} = \frac{1}{K_A Q_m} + \frac{C_e}{Q_m} \quad (2)$$

The values of K_A and Q_m are determined from the intercept and slope of the straight line in Fig. 3 for XAD-16 and XAD-7 HP. The calculated parameters of Langmuir equation were presented in Table 5.

The second isotherm was used in this study is Freundlich isotherm [20–22]:

$$q_e = K_f \cdot C_e^{1/n} \quad (3)$$

A logarithmic plot linearizes the equation enabling the exponent n and the constant K_f to be determined:

$$\ln q_e = \ln K_f + \left(\frac{1}{n}\right) \ln C_e \quad (4)$$

The values of K_f and 1/n at different concentrations were determined from the slope and intercept of the linear plots of ln q_e and ln C_e. Fig. 4 shows plot of Freundlich equation isotherm for MB adsorption for both adsorbents. Results of Freundlich equation were presented in Table 5.

Temkin isotherm [23] contains a factor that explicitly takes into the account adsorptive–adsorbent interactions. This isotherm assumes that (1) the heat of adsorption of all the molecules in the layer decreases linearly with coverage due to adsorbent-adsorbate interactions, and that (2) the adsorption is characterized by a uniform distribution of binding energies, up to some maximum binding energy:

$$q_e = \frac{RT}{b} \ln(K_T C_e) \quad (5)$$

Eq. (5) can be linearized as:

$$q_e = B_1 \ln K_T + B_1 \ln C_e \quad (6)$$

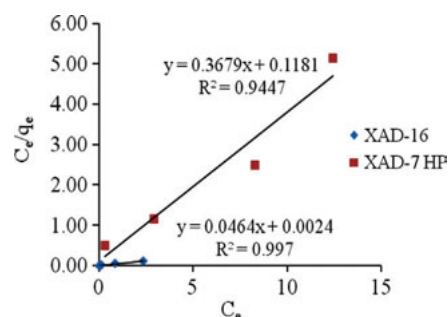


Fig. 3. Langmuir isotherm for the adsorption of MB on XAD-16 and XAD-7 HP.

Table 5
Results of adsorption isotherms for both of two adsorbents on adsorption of MB

Langmuir isotherm					
XAD-16			XAD-7 HP		
Q_m	K_A	R^2	Q_m	K_A	R^2
21.55	19.33	0.997	2.72	3.11	0.9447
Freundlich isotherm					
XAD-16			XAD-7 HP		
$\ln K_f$	$1/n$	K_f	n	R^2	
2.2214	0.5185	9.22	1.9286	0.973	
0.1317	0.4282	1.14	2.34	0.68	
Temkin isotherm					
XAD-16			XAD-7 HP		
B_1	$\ln K_T$	K_T	R^2	B_1	R^2
2.7589	4.043	57.00	0.9688	0.646	0.459

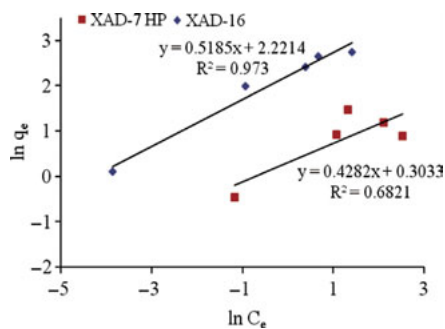


Fig. 4. Freundlich isotherms for the adsorption of MB on XAD-16 and XAD-7 HP.

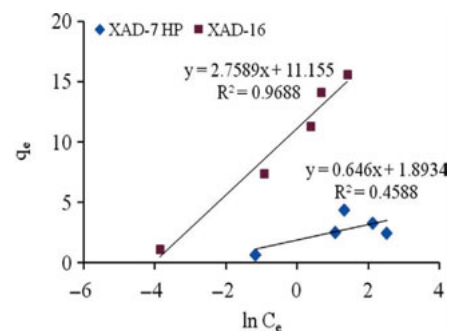


Fig. 5. Temkin isotherms for the adsorption of MB on XAD-16 and XAD-7 HP.

In Eq. (6),

$$B_1 = \frac{RT}{b} \quad (7)$$

A plot of q_e versus $\ln C_e$ enables the determination of the isotherm constants B_1 and K_T from the slope and the intercept. Fig. 5 shows the Temkin isotherm plots for both of adsorbents, and isotherm parameters were shown in Table 5.

Amberlite XAD-16 gives good results for all of isotherm with the experimental result of MB adsorption R^2 value of 0.99 except Temkin. Temkin isotherm does not obey to experimental results well.

3.4. Adsorbent characterization

FTIR spectrum of Amberlite XAD-7 HP resin were recorded before and after the MB adsorption. The spectrum was shown in Fig. 6. XAD-7 HP contains ester group O=C=O and all esters give IR bands at approximately

1700, 1200 and 1100 cm^{-1} . The strong band at 1731.24 cm^{-1} was attributed to the stretching modes of C=O bond of the ester group. The absorption band at 1260.16 cm^{-1} was due to the asymmetric stretching of the C–C and C–O bonds. The band at 1144.90 cm^{-1} was assigned to the vibration involving the ester oxygen and the next two carbons attached to it in the hydrocarbon chain. The band at 2970.43 cm^{-1} was due to the stretching mode of C–H [24]. It was observed that there is a difference between the FTIR spectrum of resins before and after the MB adsorption. We determined an additional band at 1557.97 cm^{-1} , which can be caused by a complex formed with MB adsorption onto the XAD-7 HP resin. This band might be attributed to the interaction between the protonated oxygen atom of the ester group and chloro-complex that shows the presence of MB on the resin adsorbent [24].

The broad band at around 3500 cm^{-1} was assigned to the adsorbed water and the increment of that for XAD-7 HP MB shows that adsorbed water amount was increased during the adsorption process naturally.

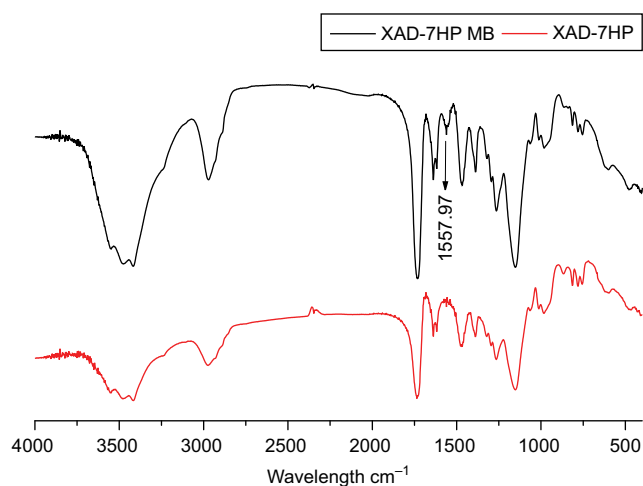


Fig. 6. FTIR spectrum of Amberlite XAD-7 HP resin before and after the adsorption.

FTIR spectrum of Amberlite XAD-16 resin were recorded before and after the MB adsorption. The spectrum was shown in Fig. 7. The spectrum exhibits a band at 2931 cm^{-1} ascribed to the stretching modes of aliphatic C–H groups. The four bands that following each other at $1605, 1513, 1487, 1445\text{ cm}^{-1}$ assigned to ring vibration of benzene rings, which also contain contribution due to bending observed at $902, 836, 794$ and 711 cm^{-1} , assigned to out of plane ring C–H bonding vibrations [25]. The FT-IR spectrum of MB adsorbed Amberlite XAD-16 in comparison with FT-IR spectrum of pure Amberlite XAD-16 depicted one additional two-necked band at 1137.15 cm^{-1} . It was attributed to the stretching modes of C–N bond that exist in the chemical structure of MB. Thereby the adsorption of MB on the two resin adsorbent

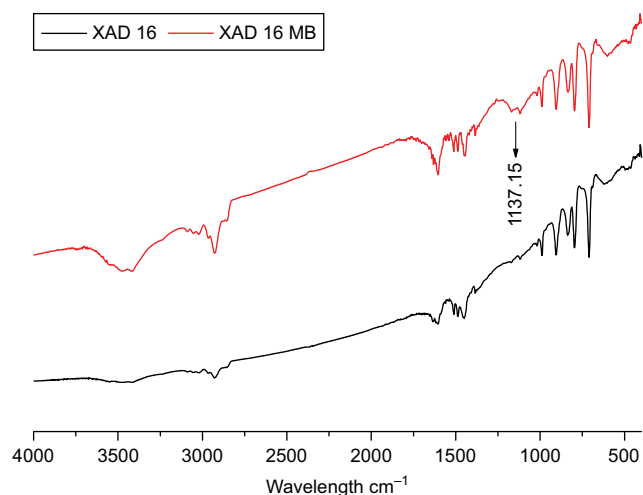


Fig. 7. FTIR spectrum of Amberlite XAD-16 resin before and after the adsorption.

Amberlite XAD-7 HP and Amberlite XAD-16 was supported by FTIR spectrum characterization.

SEM analysis shows that the XAD-16 had pores where the MB was trapped and adsorbed into these pores. Figs. 8a and b shows surface of XAD-16 before and after adsorption of MB. It has been clearly seen that the surface of XAD-16 after the adsorption trapped MB molecules nearly full.

3.5. Kinetic studies

Time of contact of adsorbent and adsorbate is of great importance in adsorption since contact time depends on the nature of the system used.

As a part of kinetic studies, the effect of contact time for the adsorption of MB by Amberlite XAD-16 and XAD-7 has been studied for a period of 32 and 27 h for initial MB concentrations of 17.36 mg l^{-1} at 298 K, respectively. Both adsorbent dosage were 0.01 g. The effect of contact time on removal of MB is shown in Tables 6 and 7 and Fig. 9. For both adsorbents uptake of adsorbate

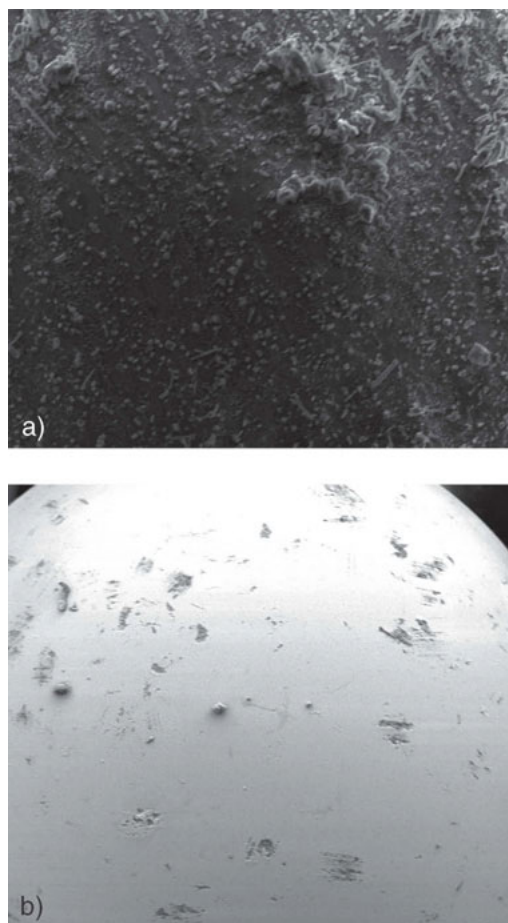


Fig. 8. SEM photo of XAD-16 (a) before and (b) after adsorption of MB.

Table 6
Effect of contact time on the adsorption of MB with XAD-16

Amount of XAD-16 (g)	C_0 (mg l ⁻¹)	C_t (mg l ⁻¹)	q_t	Removal (%)	t (h)
0.01	17.36	16.12	2.47	7.10	0.25
0.01	17.36	13.68	7.36	21.19	0.50
0.01	17.36	15.09	4.52	13.03	0.75
0.01	17.36	14.30	6.12	17.62	1.00
0.01	17.36	14.00	6.71	19.32	1.50
0.01	17.36	12.87	8.96	25.82	2.00
0.01	17.36	9.58	15.56	44.82	3.00
0.01	17.36	5.96	22.79	65.65	20.00
0.01	17.36	4.20	26.31	75.80	27.00
0.01	17.36	4.40	24.92	74.67	28.00
0.01	17.36	1.37	27.80	92.11	30.00
0.01	17.36	1.73	28.94	90.03	32.00

Table 7
Effect of contact time on the adsorption of MB with XAD-7

Amount of XAD-7 (g)	C_0 (mg l ⁻¹)	C_t (mg l ⁻¹)	q_t	Removal (%)	t (h)
0.01	17.36	16.63	1.45	4.181	0.25
0.01	17.36	16.53	1.65	4.750	0.50
0.01	17.36	16.48	1.75	5.034	0.75
0.01	17.36	16.28	2.16	6.211	1.00
0.01	17.36	16.14	2.44	7.023	1.50
0.01	17.36	16.09	2.52	7.267	2.00
0.01	17.36	15.86	2.99	8.607	4.20
0.01	17.36	15.54	3.64	10.475	20.00
0.01	17.36	15.81	3.09	8.891	27.00

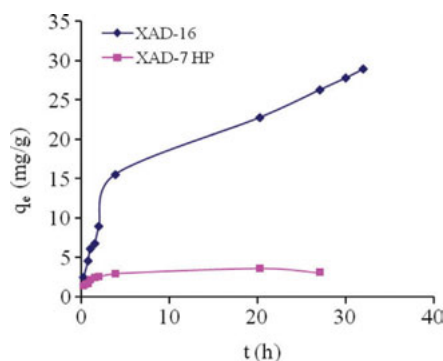


Fig. 9. Effect of contact time on the adsorption of MB.

species is fast at the initial stages of the contact period, and thereafter, it becomes slower near the equilibrium. In between these two stages of the uptake, the rate of adsorption is found to be nearly constant. This is obvious

from the fact that a large number of vacant surface sites are available for adsorption during the initial stage, and after a lapse of time, the remaining vacant surface sites are difficult to be occupied due to repulsive forces between the solute molecules on the solid and bulk phases [23].

Pseudo-second-order model [23,26]:

The equation for the pseudo-second order model is shown below:

$$\frac{dq_t}{dt} = k_s(q_e - q_t)^2 \quad (8)$$

In this equation, k_s is the pseudo-second-order rate coefficient (mg g⁻¹ min⁻¹). If Eq. (8) is integrated, a linear equation is obtained. This equation is shown followed:

$$\frac{t}{q_t} = \frac{1}{k_s q_e^2} + \frac{1}{q_e} t \quad (9)$$

The initial sorption rate, Γ (g mg⁻¹ min⁻¹), at $t \rightarrow 0$ is defined as:

$$\Gamma = k_s q_e^2 \quad (10)$$

The values of k_s and calculated q_e are obtained from the slope of the plot t/q_t versus t . Γ and k_s are obtained from the intercept. The pseudo-second-order model parameters were shown in Table 8 and plots of both adsorbents can be seen from Fig. 10.

The Elovich equation:

The Elovich model equation [27] is generally expressed as:

$$\frac{dQ}{dt} = \alpha \cdot \exp(-\beta \cdot Q) \quad (11)$$

where α is the initial adsorption rate (mg g⁻¹ min⁻¹) and β is the desorption constant (g mg⁻¹) during any one experiment. To simplify the Elovich equation, $\alpha\beta t \gg 1$ is assumed and by applying the boundary conditions $Q = 0$ at $t = 0$ and $Q = Q$ at $t = t$ equation becomes:

$$Q = \frac{1}{\beta} \ln(\alpha\beta) + \frac{1}{\beta} \ln(t) \quad (12)$$

A plot of q_t versus $\ln(t)$ should yield a linear relationship with a slope of $(1/\beta)$ and an intercept of $(1/\beta) \ln(\alpha\beta)$ (Fig. 11). The constants are listed in Table 8.

Weber and Morris intra-particle diffusion model:

Intra-particle diffusion can be estimated by using the Weber–Morris intraparticle diffusion model [23,28],

$$q_t = k_{id} t^{1/2} + I \quad (13)$$

In Eq. (13), k_{id} is the intra-particle diffusion rate coefficient and I gives an idea about the thickness of the boundary layer. These values can be found by a plot, q_t

Table 8
Results of rate models for both adsorbents on adsorption of MB

Elovich model					
XAD-16			XAD-7 HP		
α	β	R^2	α	β	R^2
22	0.18	0.957	54	2.30	0.892
Pseudo second order model					
XAD-16				XAD-7 HP	
q_e (mg.g ⁻¹)	Γ (g mg ⁻¹ min ⁻¹)	k_s (mg g ⁻¹ min ⁻¹)	R^2	q_e	R^2
30.21	0.13	1.42×10^{-4}	0.986	3.32	0.991
W-M Intra particle diffusion model					
XAD-16			XAD-7 HP		
k_{id} (mg.g ⁻¹ min ^{-1/2})	I (mg.g ⁻¹)	R^2	k_{id} (mg.g ⁻¹ min ^{-1/2})	I (mg.g ⁻¹)	R^2
0.59	2.13	0.970	0.047	1.71	0.717

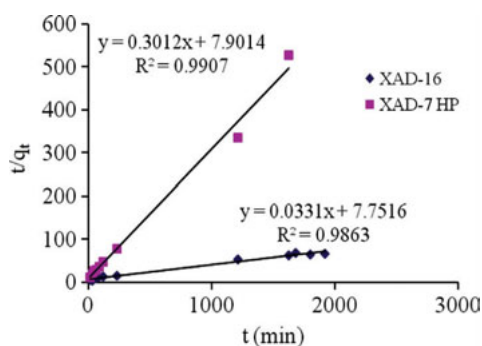


Fig. 10. Pseudo-second order model for both of two adsorbents.

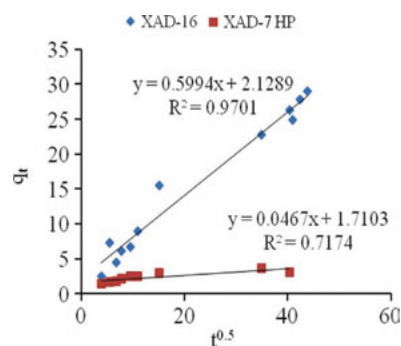


Fig. 12. Weber–Morris diffusion model for both of two adsorption.

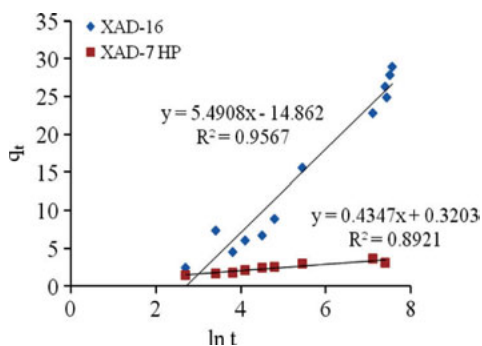


Fig. 11. Elovich model for both of two adsorption.

versus $t^{1/2}$ The slope is k_{id} and the intercept is I . As seen in Fig. 12, the straight lines deviate from the origin. The difference between final mass transfer rate and initial mass transfer rate may cause the deviations of straight lines. I and k_{id} values are shown in Table 8.

In this study, all of rate models which were applied to kinetic data were compared with the correlation coef-

ficients of both adsorbents. As a result of these rate models, the correlation coefficients of pseudo-second-order model was closer unity than other models. The correlation coefficient for XAD-16 is 0.98 and for XAD-7 HP is 0.99. Therefore, the adsorption of MB on Amberlite XAD-16 and XAD-7 HP is fitted to pseudo-second-order kinetic model.

4. Conclusions

This study shows that investigation of adsorption MB from wastewater stream using XAD-16 and XAD-7 HP is applicable. XAD-16 is more effective adsorbent than XAD-7 HP in light of experimental results. In similar conditions, 99.48% of MB was removed by XAD-16 but only 59.76% of MB was removed by XAD-7 HP from wastewater. Elovich, pseudosecond order and W-M diffusion models were tried to fit experimental kinetic results. Pseudosecond order model showed good result with R^2 value over than 0.99. Temkin, Freundlich

and Langmuir isotherms were applied to equilibrium data. Langmuir isotherm was fitted more than other isotherms. FTIR and SEM analysis shows that the adsorbents kept MB on their surface and pours strongly.

Acknowledgements

This work was studied in Beykent University laboratories. We are grateful to The Board of Trustees of Beykent University for supplied chemicals and other equipment. We would like to thank İstanbul University Chemical Engineering Department for SEM analysis (DPT 2008K121000) and FTIR analysis.

We would like to thank İstanbul University Chemical Engineering Department for FTIR and SEM analysis.

Symbols

C_0	—	initial concentration of methylene blue in aqueous solution, mg l^{-1}
C_e	—	concentration of methylene blue at adsorption equilibrium, mg l^{-1}
C_t	—	concentration of methylene blue at any time t , mg l^{-1}
q_e	—	the amount of adsorbed methylene blue per gram of adsorbent at equilibrium, mg g^{-1}
q_t	—	the amount of adsorbed methylene blue per gram of adsorbent at any time t , mg g^{-1}
W	—	mass of the adsorbent, g
V	—	volume of the aqueous solution used in adsorption, l
k_s	—	pseudo-second-order rate coefficient, $\text{mg}\cdot\text{g}^{-1}\cdot\text{min}^{-1}$
k_{id}	—	intra-particle diffusion rate constant, $\text{mg}\cdot\text{g}^{-1}\cdot\text{min}^{-1/2}$
$t^{1/2}$	—	the half adsorption time of dye, $\text{min}^{1/2}$
R^2	—	linear regression coefficient

References

- [1] S.A. Cárdenas, T.G. Velázquez, G.O. Revilla, M.S.L. Cortéz and B.G. Perea, Adsorption of phenol and dichlorophenols from aqueous solutions by porous clay heterostructure (PCH), *J. Mex. Chem. Soc.*, 49 (2005) 287–291.
- [2] S. Altenor, B. Carene, E. Emmanuel, J. Lambert, J.J. Ehrhardt and S. Gaspard Adsorption studies of methylene blue and phenol onto vetiver roots activated carbon prepared by chemical activation, *J. Hazard. Mater.*, 165 (2009) 1029–1039.
- [3] N.M. Mahmoodi, M. Arami and K. Gharanjig, Laboratory studies and CFD modeling of photocatalytic degradation of colored textile wastewater by titania nanoparticles, *Desalin. Water Treat.*, 1 (2009) 312–317.
- [4] E. Forgacs, T. Cserhati, and G. Oros, Removal of synthetic dyes from wastewaters: a review, *Environ. Int.*, 30 (2004) 953–971.
- [5] U.G. Akpan and B.H. Hameed, Parameters affecting the photocatalytic degradation of dyes using TiO_2 -based photocatalysts: a review, *J. Hazard. Mater.*, 170 (2009) 520–529.
- [6] R.L. Tseng, F.C. Wu and R.S. Juang, Liquid-phase adsorption of dyes and phenols using pinewood-based activated carbons, *Carbon*, 41 (2003) 487–495.
- [7] F.C. Wu, R. Tseng and R.S. Juang, Preparation of highly microporous carbons from fir wood by KOH activation for adsorption of dyes and phenols from water, *Sep. Purif. Technol.*, 47 (2005) 10–19.
- [8] X. Zhang, A. Li, Z. Jiang and Q. Zhang, Adsorption of dyes and phenol from water on resin adsorbents: effect of adsorbate size and pore size distribution, *J. Hazard. Mater.*, B137 (2006) 1115–1122.
- [9] N. Kannan and M.M. Sundaram, Kinetics and mechanism of removal of methylene blue by adsorption on various carbons—a comparative study, *Dyes Pigm.*, 51 (2001) 25–40.
- [10] D. Ghosh and K.G. Bhattacharyya, Adsorption of methylene blue on kaolinite, *Appl. Clay Sci.*, 20 (2002) 295–300.
- [11] M. Doğan, Y. Özdemir and M. Alkan, Adsorption kinetics and mechanism of cationic methyl violet and methylene blue dyes onto sepiolite, *Dyes Pigm.*, 75 (2007) 701–713.
- [12] M. Doğan, M. Alkan, A. Türkyilmaz and Y. Özdemir, Kinetics and mechanism of removal of methylene blue by adsorption onto perlite, *J. Hazard. Mater.*, B109 (2004) 141–148.
- [13] R. Han, J. Zhang, P. Han, Y. Wang, Z. Zhao and M. Tang, Study of equilibrium, kinetic and thermodynamic parameters about methylene blue adsorption onto natural zeolite, *Chem. Eng. J.*, 145 (2009) 496–504.
- [14] C.A.P. Almeida, N.A. Debacher, A.J. Downs, L. Cottet and C.A.D. Mello, Removal of methylene blue from colored effluents by adsorption on montmorillonite clay, *J. Colloid Interface Sci.*, 332 (2009) 46–53.
- [15] S. Hong, C. Wen, J. He, F. Gan and Y.S. Ho, Adsorption thermodynamics of methylene blue onto bentonite, *J. Hazard. Mater.*, 167 (2009) 630–633.
- [16] D.A. Fungaro, M. Bruno and L.C. Grosche, Adsorption and kinetic studies of methylene blue on zeolite synthesized from fly ash, *Desalin. Water Treat.*, 2 (2009) 231–239.
- [17] J.X. Lin and L. Wang, Treatment of textile wastewater using organically modified bentonite, *Desalin. Water Treat.*, 25 (2011) 25–30.
- [18] I. Langmuir, Constitution and fundamental properties of solids and liquids, *J. Am. Chem. Soc.*, 38 (1916) 2221–2295.
- [19] S. Azizian, M. Haerifar and H. Bashiri, Adsorption of methyl violet onto granular activated carbon: equilibrium, kinetics and modeling, *Chem. Eng. J.*, 146 (2009) 36–41.
- [20] H. Freundlich, Über die adsorption in losungen, *Z. Phys. Chem.*, 57 (1906) 385–470.
- [21] A.R. Iftikhar, H.N. Bhatti, M.A. Hanif. and R. Nadeem, Kinetic and thermodynamic aspects of Cu(II) and Cr(III) removal from aqueous solutions using rose waste biomass, *J. Hazard. Mater.*, 161 (2009) 941–947.
- [22] N.P. Couturin, S. Altenor, D. Cossement, C.J. Marius and S. Gaspard, Comparison of parameters calculated from the BET and Freundlich Isotherms obtained by nitrogen adsorption on activated carbons: a new method for calculating the specific surface area, *Microporous Mesoporous Mater.*, 111, (2008) 517–522.
- [23] R.K. Rajoriya, B. Prasad, I.M. Mishra and K.L. Wasewar, Adsorption of Benzaldehyde on Granular activated carbon: kinetics, equilibrium, and thermodynamic, *Chem. Biochem. Eng. Q.*, 21(3) (2007) 219–226.
- [24] N.V. Nguyen, J.C. Lee, S.K. Kim, M.K. Jha, K.S. Chung and J. Jeong, Adsorption of gold(III) from waste rinse water of semiconductor manufacturing industries using Amberlite XAD-7HP resin, *Gold Bull.*, 43(3) (2010) 200–208.
- [25] M. Merdivan, M.Z. Düz and C. Hamamci, Sorption behaviour of uranium(VI) with *N,N*-dibutyl-*N*-benzoylthiourea Impregnated in Amberlite XAD-16, *Talanta*, 55 (2001) 639–645.
- [26] S. Azizian, Kinetic models of sorption: a theoretical analysis, *J. Colloid Interface Sci.*, 276 (2004) 47–52.
- [27] K. Urano and H. Tachikawa, Process development for removal and recovery of phosphorus from wastewater by a new adsorbent. II. Adsorption rates and breakthrough curves, *Ind. Eng. Chem. Res.*, 30 (1991) 1897–1899.
- [28] C. Costa and A. Rodrigues, Intraparticle diffusion of phenol in macroreticular adsorbents: modeling and experimental study of batch and CSTR adsorbents, *Chem. Eng. Sci.*, 40 (1985) 983–993.